MultiCraft

International Journal of Engineering, Science and Technology
Vol. 11, No. 2, 2019, pp. 1-20

INTERNATIONAL JOURNAL OF ENGINEERING, SCIENCE AND TECHNOLOGY

www.ijest1-ng.com
www.ajol.info/index.php/ijest

A protection technique for series capacitor compensated 400 kV double circuit transmission line based on wavelet transform including inter-circuit and cross-country faults

Gaurav Kapoor

Department of Electrical Engineering, Modi Institute of Technology, Kota, Rajasthan, INDIA
Corresponding Author: e-mail: gaurav.kapoor019@gmail.com, Mobile: +91-9166868988

Abstract

In this paper, wavelet transform based technique is introduced to detect and classify the faults in a series capacitor compensated double circuit transmission line. The three phase currents of both circuits measured at only one end of the series compensated double circuit transmission line are used to calculate the approximate and high frequency detail coefficients including wavelet energy content of each phase current signal. To evaluate the performance of proposed fault detection technique, simulation studies have been carried out on a series capacitor compensated double circuit transmission line test system. The major advantage of this proposed scheme is that it offers protection to entire transmission line length using one end fault current data only. The test results prove that all types of faults are correctly detected and the faulty phase is accurately identified using proposed technique. This technique is robust to the variation in fault type, fault inception time, fault resistance, ground resistance and fault location.

Keywords: Fault detection, fault classification, series capacitor compensated double circuit transmission line, wavelet transform.

DOI: http://dx.doi.org/10.4314/ijest.v11i2.1

1. Introduction

The continuous operation of a transmission line is reliant on a perfect fault detection and location technique. A perfect fault detector decreases the interruption and aids in the fast restoration of electricity. Many methods of fault detection and classification have been proposed till now for the protection of series capacitor compensated double circuit transmission line. The review of some literatures has been discussed in this section. Hilbert Huang transform based online differential relay has been developed and used for the protection of STATCOM compensated three phase transmission line against internal faults, external faults, cross country faults and faults with variation in fault inception angle and source impedance (Biswal *et al*., 2018). Wavelet transform energy has been utilized for fault detection and classification in a fixed TCSC compensated three phase transmission line (Biswas *et al*., 2018). MDFT has been used as a very effective tool for fault detection and localization in double circuit transmission line (Gaur and Bhalja, 2018). Wavelet transform has been used for fault detection and classification in a 400 kV series capacitor compensated double circuit transmission line (Gautam *et al.*, 2018). Fault detection in a series capacitor compensated double circuit transmission line using wavelet transform has been reported in (Gautam *et al.*, 2018). Continuous wavelet transform is applied for the differential protection of transmission line (Govar and Seyedi, 2016). Location of faults on series compensated double circuit transmission line using distributed parameter transmission line model has been described in (Kang *et al*., 2015). Mathematical morphology has been used as a very helpful tool for fault detection in a double circuit transmission line (Kapoor, 2018). Wavelet transform in conjunction with artificial neural network has been utilized for fault detection, classification and location in transmission line (Koley *et al*., 2016). Wavelet transform is applied for fault detection in a series capacitor compensated three phase transmission line (Kapoor, 2018). Wavelet transform based protection scheme has been used for double circuit

transmission lines (Kapoor, 2018). Support vector machine in combination with artificial neural network is used for the protection of three phase transmission line (Koley *et al*., 2017).

Recently, the one terminal travelling wave based cross differential protection technique has also been used for the protection of double circuit transmission line (Monteiro *et al*., 2018). Fault location in STATCOM compensated double circuit transmission line using artificial neural network has been presented in (Nagam *et al.*, 2017). Naïve Bayes classifier has also been used as a very efficient tool for the protection of parallel transmission lines (Swetapadma and Yadav, 2016). Artificial neural network has been utilized for fault classification and location in double circuit transmission line (Saravanan and Rathinam, 2012). Artificial neural network has been used as a very useful tool for fault detection, classification and location in parallel transmission line (Swetapadma and Yadav, 2016). Artificial neural network based protection technique has been presented for double circuit transmission line protection (Yadav and Swetapadma, 2014).

The proposed work reports a single ended fault detection technique for series capacitor compensated double circuit transmission line against different types of shunt faults including boundary faults, inter-circuit and cross-country faults with varying various fault parameters. The paper is organized as follows: the schematic of series capacitor compensated double circuit transmission line is depicted in section-2. The process of feature extraction from the current signals of both circuits using wavelet transform is presented in section-3. Simulation results are analyzed in section-4. Finally, the conclusions of the work are drawn in section-5.

2. Power System Specifications

The schematic of double circuit transmission line compensated with series capacitor under simulation is depicted in Figure 1. The test system consists of a 400 kV, 50 Hz double circuit transmission line of 200 km length. The double circuit transmission line is connected to a 400 kV source at the sending end and two loads each of 100 MW and 100 MVAr at the receiving end. The series capacitors are connected at the mid-point of the double circuit transmission line. The relay is installed at bus-1 to protect the total length of a double circuit transmission line which can be seen in Figure 1. The double circuit transmission line model is simulated using MATLAB. Feature extraction of the fault current signals of both circuits has been done using daubechies-4 mother wavelet to calculate the approximate and detail coefficients.

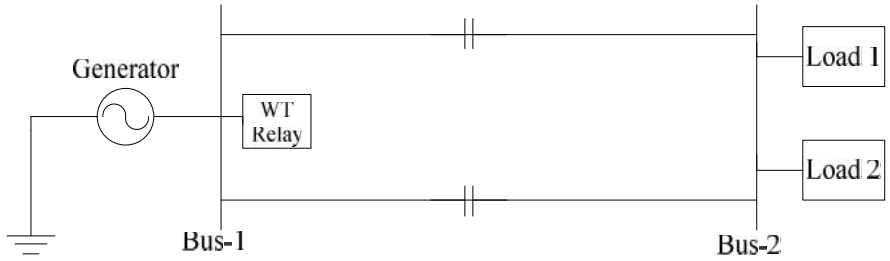

Figure 1. Schematic of proposed simulation model

3. Proposed Fault Detection and Classification Technique

In a digital signal processing area, the schemes based on wavelet transform have become one of the most influential tools and these strategies became contemporary. As a substitute to short time Fourier transforms (STFT), the wavelet transform (WT) was developed to ascend above the shortcomings associated to its resolution problem.

Wavelet transform (Gautam *et al*., 2018) is defined as:

$$W(j, k) = \sum_j \sum_k x(k)\, 2^{-j/2}\, \varphi(2^{-j}n-k) \quad (1)$$

where, a mother wavelet is designated as φ (t) having finite energy.

High pass filter gain after double sub-sampling is defined as:

$$y_H(k) = \sum_n x(n) g(2k-n) \quad (2)$$

Low pass filter gain after double sub-sampling is defined as:

$$y_L(k) = \sum_n x(n) h(2k-n) \quad (3)$$

The various stages of the proposed technique as shown in Figure 2 are described in detail hereafter.

Step 1 Simulate the test system and generate post fault three phase current signals of both circuits.
Step 2 Analyze the three phase current signals of both circuits using wavelet transform for feature extraction.
Step 3 Calculate the magnitude of wavelet energy for each fault current signal.
Step 4 Estimate the approximate and detail coefficients of fault current signals at level-1.

Step 5 If the magnitude of detail coefficients of the faulted phase is greater than the magnitude of detail coefficients of un-faulted phase, then fault else no fault, go to step 1.

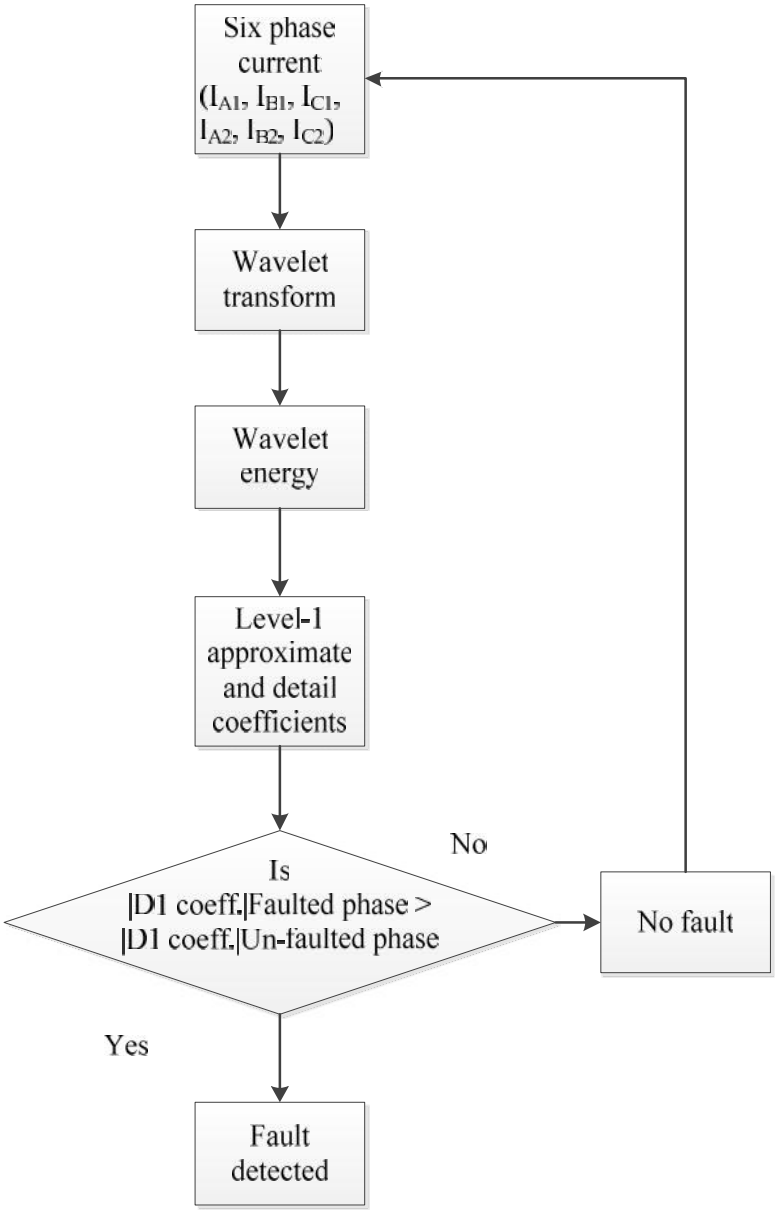

Figure 2. Schematic of proposed technique

4. Results and Discussion

To authenticate the effectiveness of the proposed fault detection/ classification technique, simulation studies have been carried out for numerous types of faults, including inter-circuit, cross-country and boundary faults. The performance of the proposed technique was investigated with variation in fault type, fault resistance, ground resistance, fault inception time and fault location. Following the fault detection and faulty phase identification, some of the simulation results are discussed in the successive subsections.

4.1 Performance During No-Fault: The performance of the proposed technique is analyzed during no-fault simulation of a test system. The three phase current of circuit-1 and circuit-2 for the duration of no-fault are shown in Figure 3. The approximate-1 and detail-1 coefficients of three phase current of circuit-1 and circuit-2 for no-fault period can be seen in Figures 4-7. The performance of wavelet transform based fault detection scheme is examined for no-fault operation and the test results are demonstrated in Table 1.

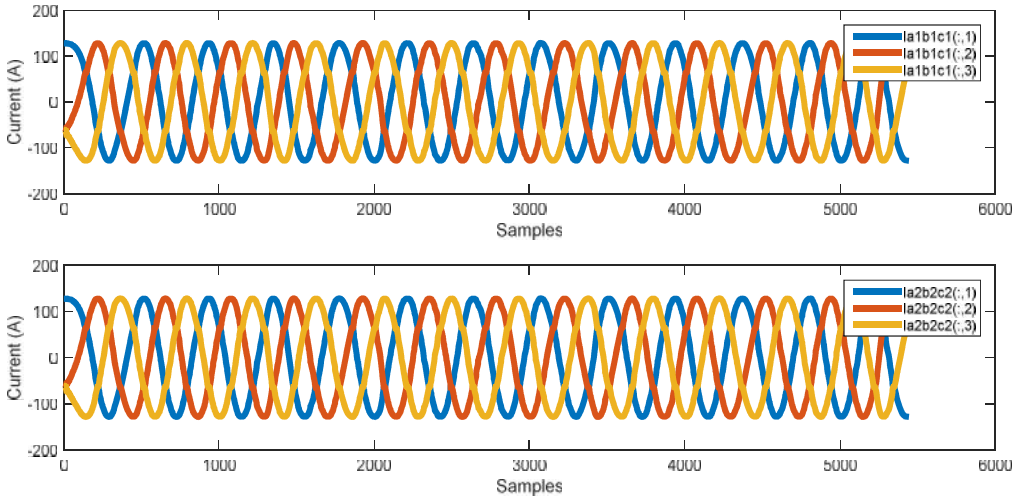

Figure 3. Three phase current of circuit-1 and circuit-2 during no-fault

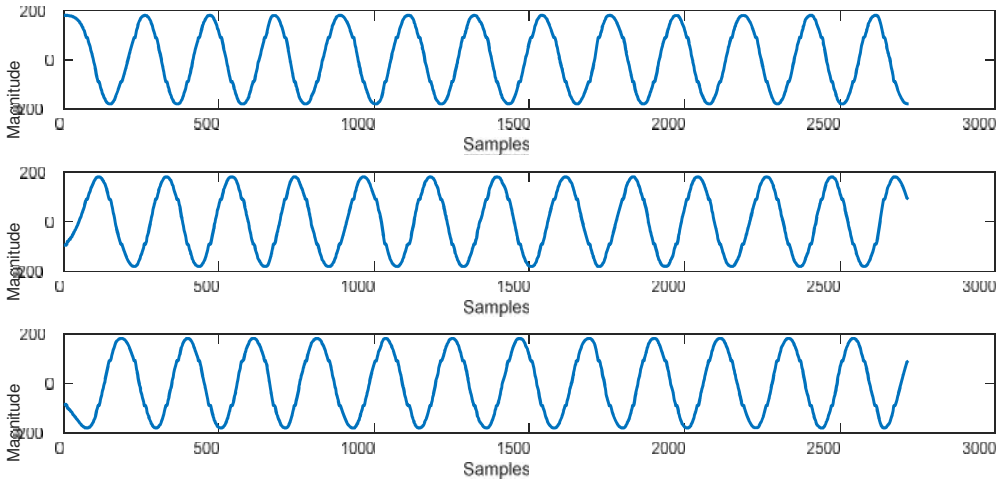

Figure 4. Approximate-1 coefficient of three phase current of circuit-1 during no fault

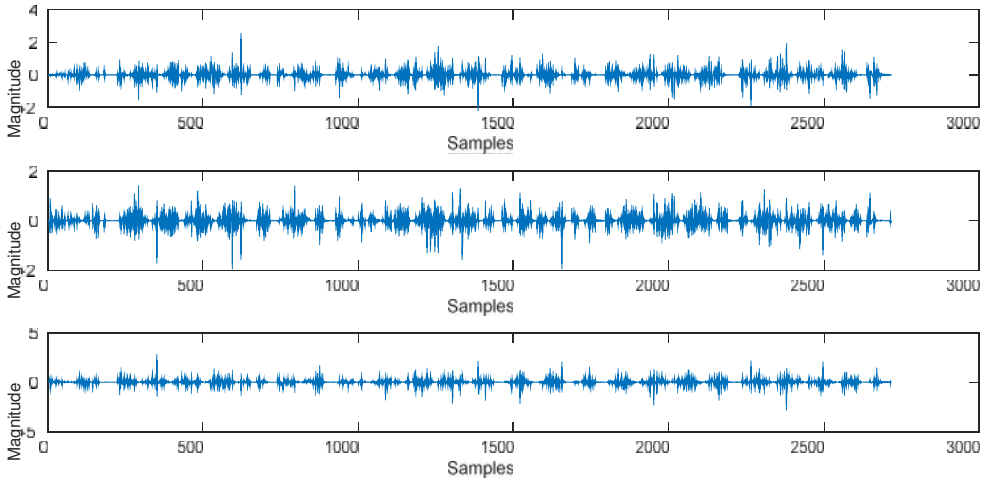

Figure 5. Detail-1 coefficient of three phase current of circuit-1 during no fault

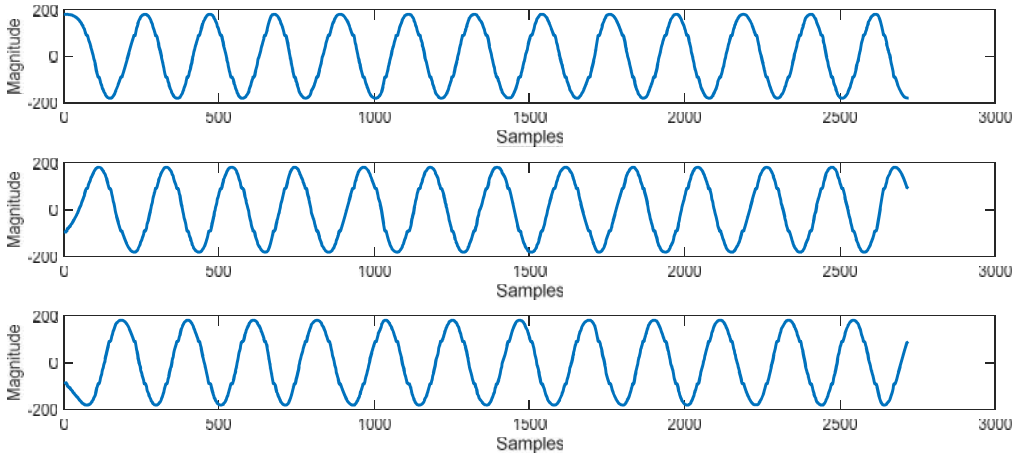

Figure 6. Approximate-1 coefficient of three phase current of circuit-2 during no fault

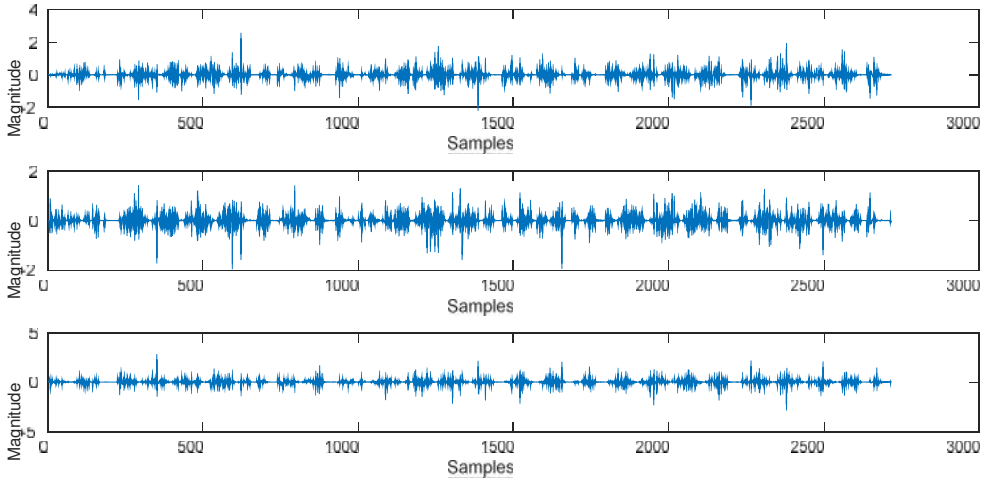

Figure 7. Detail-1 coefficient of three phase current of circuit-2 during no fault

Table 1. Test results of WT for no-fault

Phase	Output		
	Approx. Coefficient	**Detail Coefficient**	**Wavelet Energy**
A1	181.2243	2.2282	99.9294
B1	181.2682	1.1988	99.9158
C1	181.1921	2.2553	99.9198
A2	181.2231	2.2280	99.9294
B2	181.2726	1.2042	99.9157
C2	181.1520	2.2625	99.9198

4.2 Effect of Varying Fault Resistance: The performance of the proposed fault detector is investigated for various types of fault cases with varying fault resistance. The three phase current of circuit-1 and circuit-2 for the duration of phase-'B1A2C2-g' fault at 50% from bus-1 at FIT=0.1 seconds with R_f = 10 and R_g = 0.001 are shown in Figure 8. The approximate-1 and detail-1 coefficients of three phase current of circuit-1 and circuit-2 for phase-'B1A2C2-g' fault can be seen in Figures 9-12. From the simulation result as depicted in Table 2, it can be seen that the proposed technique correctly detects the fault and identifies the faulty phase and is robust to the variation in fault resistance.

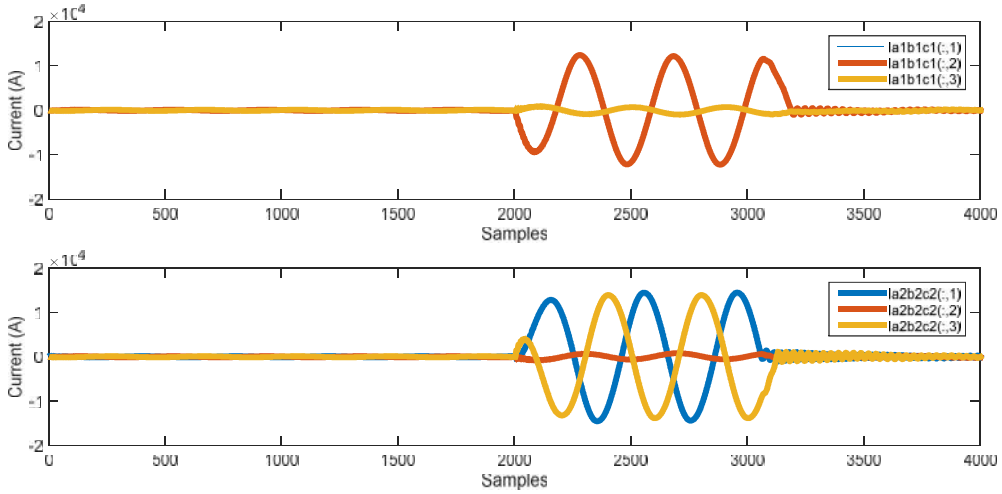

Figure 8. Three phase current of circuit-1 and circuit-2 during phase-'B1A2C2-g' fault at 50% from bus-1 at FIT=0.1 seconds with $R_f = 10$ and $R_g = 0.001$

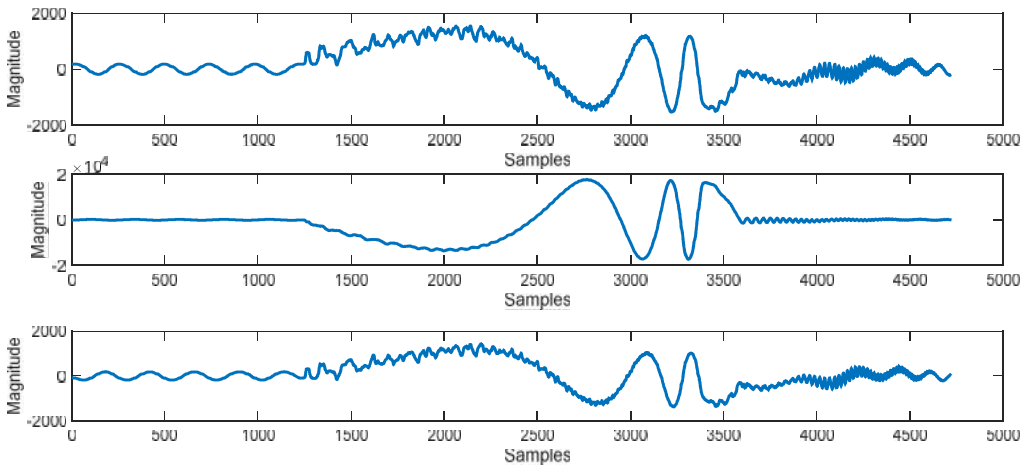

Figure 9. Approximate-1 coefficient of three phase current of circuit-1 during phase- 'B1A2C2-g' fault at 50% from bus-1 at FIT=0.1 seconds with $R_f = 10$ and $R_g = 0.001$

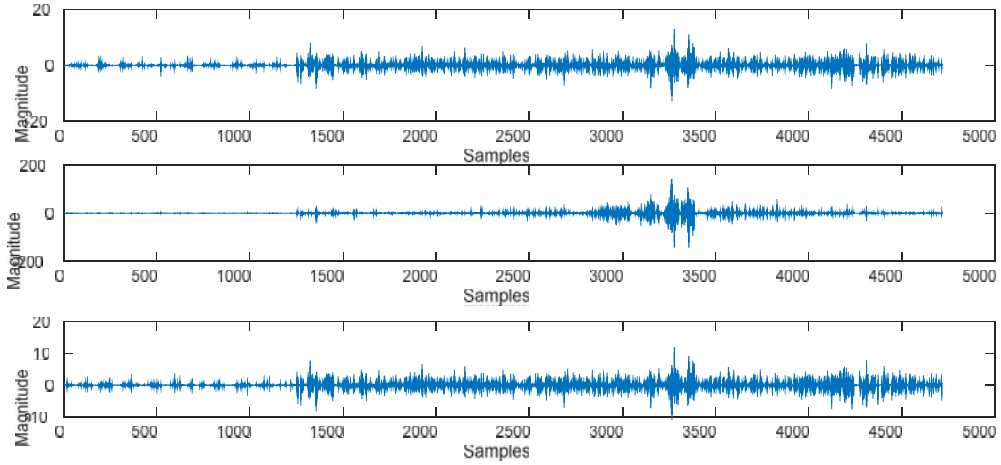

Figure 10. Detail-1 coefficient of three phase current of circuit-1 during phase- 'B1A2C2-g' fault at 50% from bus-1 at FIT=0.1 seconds with $R_f = 10$ and $R_g = 0.001$

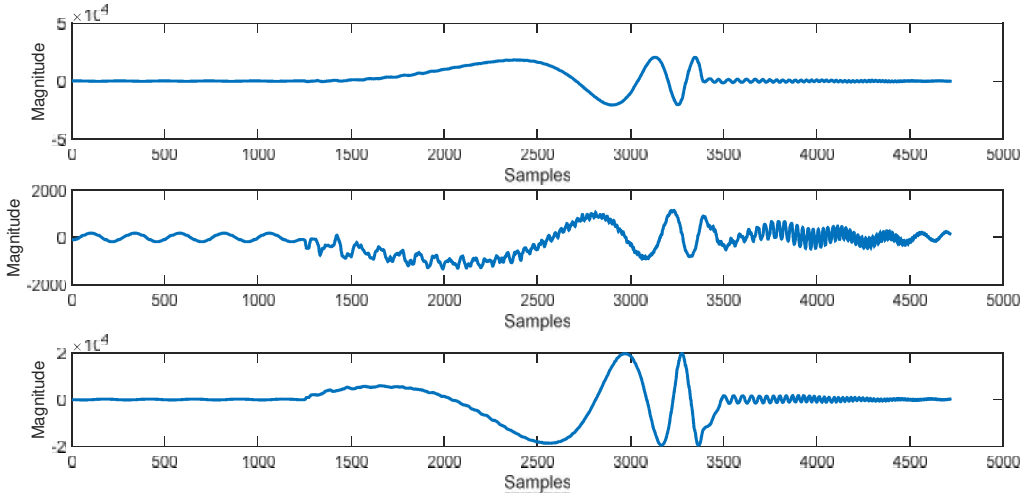

Figure 11. Approximate-1 coefficient of three phase current of circuit-2 during phase- 'B1A2C2-g' fault at 50% from bus-1 at FIT=0.1 seconds with $R_f = 10$ and $R_g = 0.001$

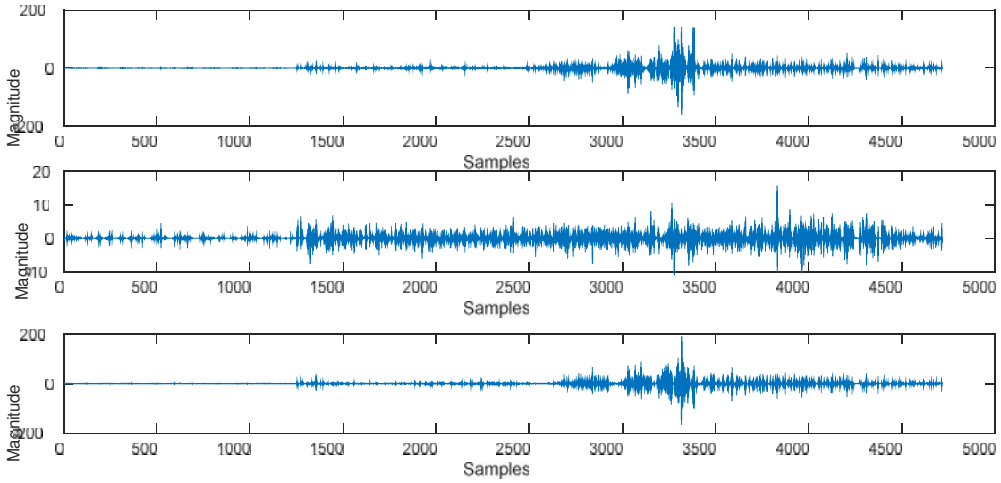

Figure 12. Detail-1 coefficient of three phase current of circuit-2 during phase- 'B1A2C2-g' fault at 50% from bus-1 at FIT=0.1 seconds with $R_f = 10$ and $R_g = 0.001$

Table 2. Test results of WT for phase-'B1A2C2-g' fault at 50% from bus-1 at FIT=0.1 seconds with $R_f = 10$ and $R_g = 0.001$

Phase	Output		
	Approx. Coefficient	Detail Coefficient	Wavelet Energy
A1	1.5419*10^3	10.9896	99.3621
B1	**1.7775*10^4**	**120.2243**	**99.9645**
C1	1.4353*10^3	10.2757	99.1583
A2	**2.0489*10^4**	**122.3651**	**99.9383**
B2	1.1429*10^3	14.0932	97.3431
C2	**1.9703*10^4**	**168.8253**	**99.9000**

4.3 Effect of Varying Ground Resistance: The performance of the proposed fault detector is investigated for various types of fault cases with variation in ground resistance. The three phase current of circuit-1 and circuit-2 for the duration of phase-'A1C1B2-g' fault at 50% from bus-1 with $R_g = 20$, $R_f = 0.001$ and FIT = 0.15 seconds are depicted in Figure 13. The approximate-1 and detail-1 coefficients of three phase current of circuit-1 and circuit-2 for phase-'A1C1B2-g' fault can be seen in Figures 14-17. From the simulation result as depicted in Table 3, it can be seen that the proposed method is not affected by variation in ground resistance and effectively detects the fault and classifies the faulty phases efficiently.

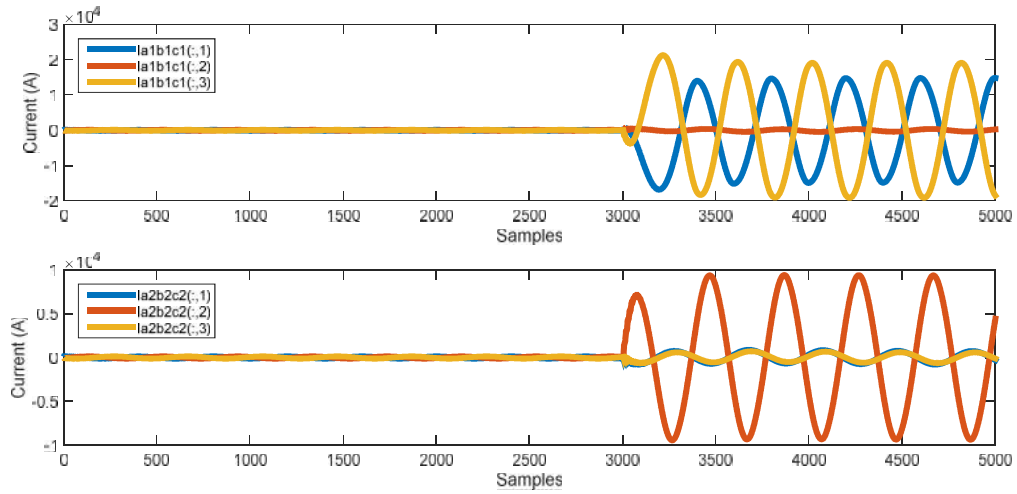

Figure 13. Three phase current of circuit-1 and circuit-2 during phase-'A1C1B2-g' fault at 50% from bus-1 with $R_g = 20$, $R_f = 0.001$ at FIT = 0.15 seconds

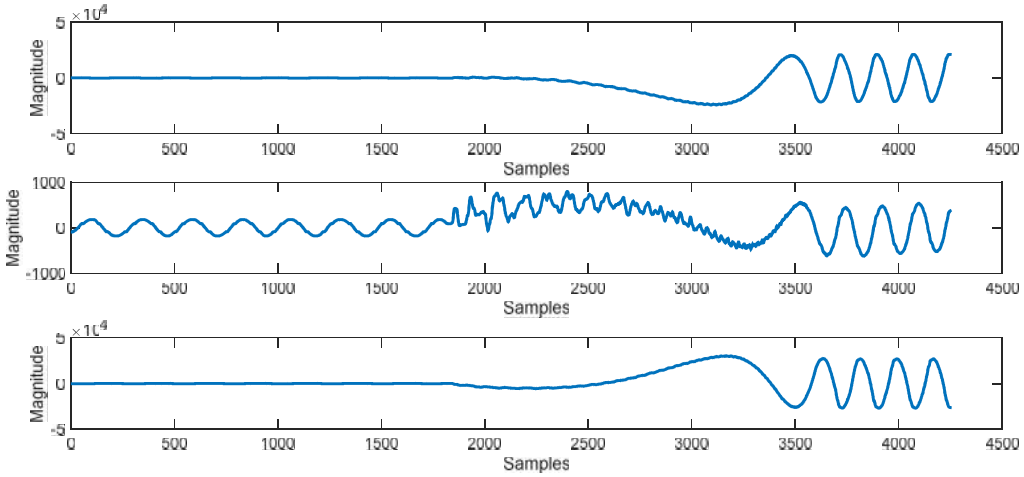

Figure 14. Approximate-1 coefficient of three phase current of circuit-1 during phase- 'A1C1B2-g' fault at 50% from bus-1 with $R_g = 20$, $R_f = 0.001$ at FIT = 0.15 seconds

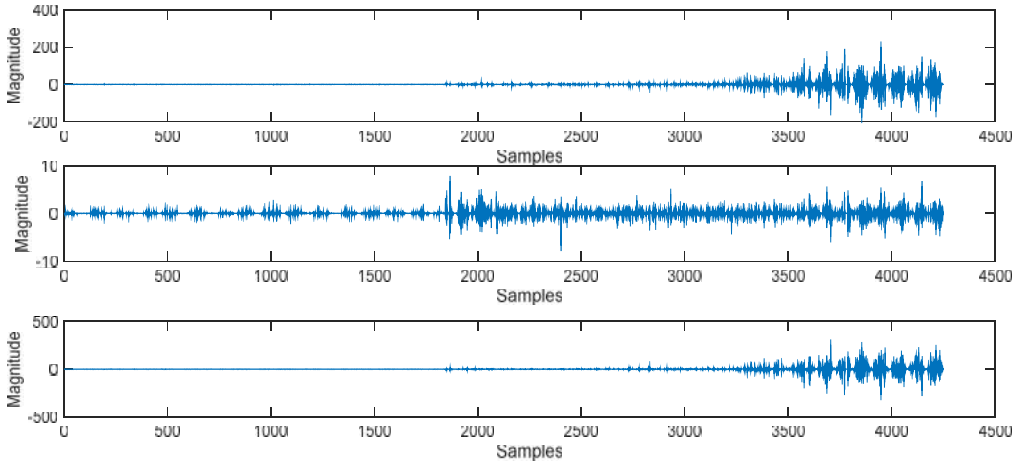

Figure 15. Detail-1 coefficient of three phase current of circuit-1 during phase- 'A1C1B2-g' fault at 50% from bus-1 with $R_g = 20$, $R_f = 0.001$ at FIT = 0.15 seconds

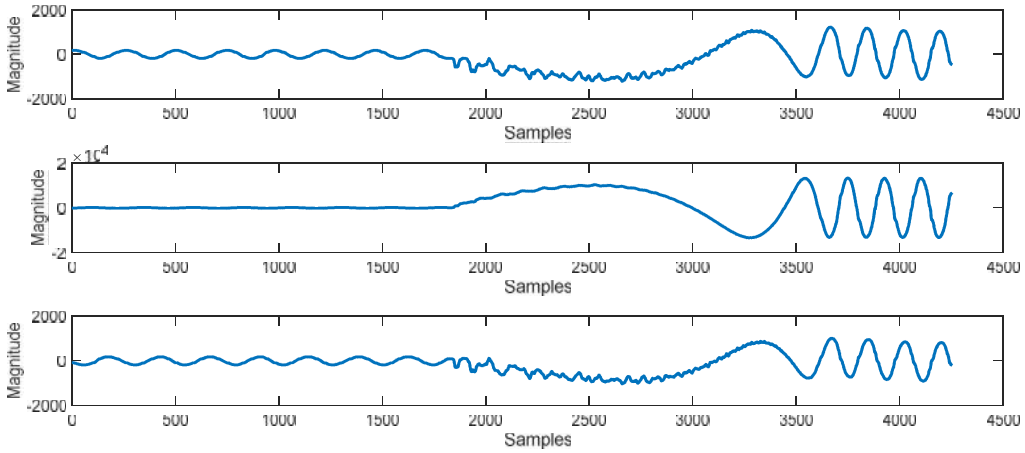

Figure 16. Approximate-1 coefficient of three phase current of circuit-2 during phase- 'A1C1B2-g' fault at 50% from bus-1 with $R_g = 20$, $R_f = 0.001$ at FIT = 0.15 seconds

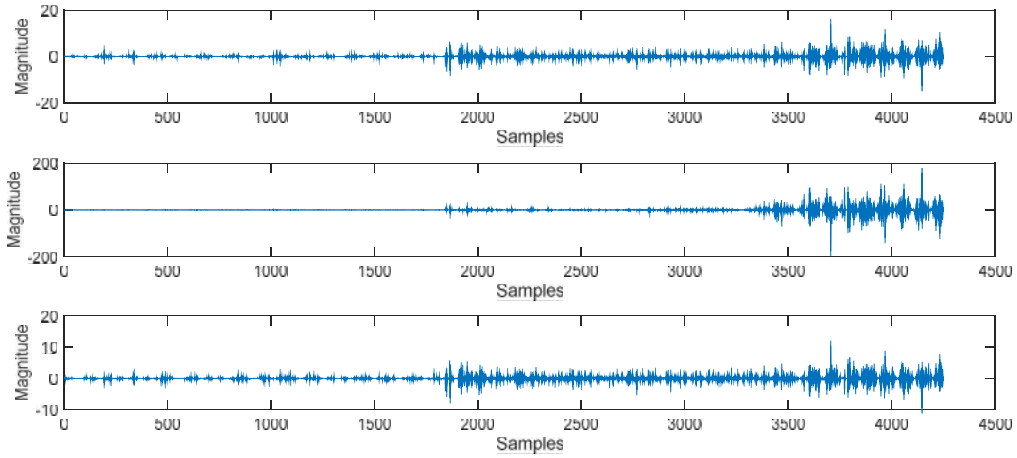

Figure 17. Detail-1 coefficient of three phase current of circuit-2 during phase- 'A1C1B2-g' fault at 50% from bus-1 with $R_g = 20$, $R_f = 0.001$ at FIT = 0.15 seconds

Table 3. Test results of WT for phase-'A1C1B2-g' fault at 50% from bus-1 at FIT = 0.15 seconds with $R_g = 20$, $R_f = 0.001$

Phase	Output		
	Approx. Coefficient	**Detail Coefficient**	**Wavelet Energy**
A1	**2.1023*10^4**	**201.0956**	**99.9740**
B1	795.4028	6.6883	99.5689
C1	**3.0564*10^4**	**253.1951**	**99.9690**
A2	1.2343*10^3	13.9353	99.8443
B2	**1.3318*10^4**	**156.6560**	**99.9520**
C2	1.0097*10^3	10.4439	99.7645

4.4 Effect of Varying Fault Inception Time: The performance of the proposed technique has been checked for variation in fault inception time. The three phase current of circuit-1 and circuit-2 during phase-'C1-g' fault at 50% from bus-1 at FIT= 0.05 seconds, $R_g = 5$ and $R_f = 2$ are depicted in Figure 18. The approximate-1 and detail-1 coefficients of three phase current of circuit-1 and circuit-2 for phase-'C1-g' fault can be seen in Figures 19-22. Table 4 presents the simulation result corresponding to the fault case simulated at 50% with fault resistance of 2 at FIT=0.05 seconds for phase-'C1-g' fault, respectively. The simulation result follows the immunity of the proposed fault detection and identification technique to the deviation in fault inception time.

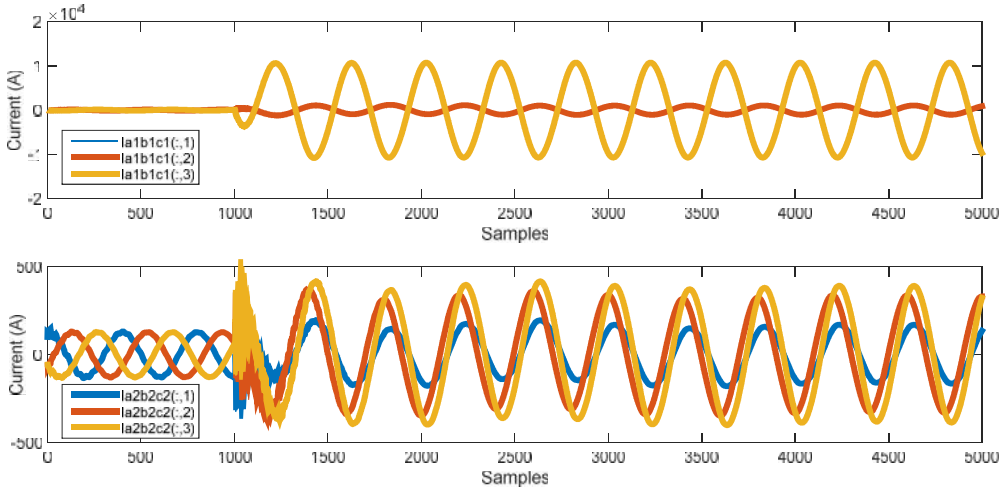

Figure 18. Three phase current of circuit-1 and circuit-2 during phase-'C1-g' fault at 50% from bus-1 at FIT= 0.05 seconds, R_g = 5 and R_f = 2

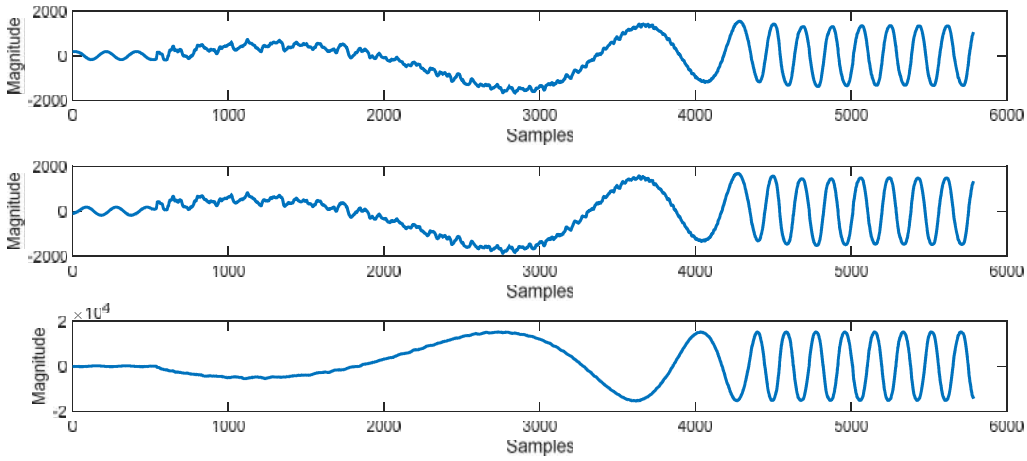

Figure 19. Approximate-1 coefficient of three phase current of circuit-1 during phase- 'C1-g' fault at 50% from bus-1 at FIT=0.05 seconds, R_g = 5 and R_f = 2

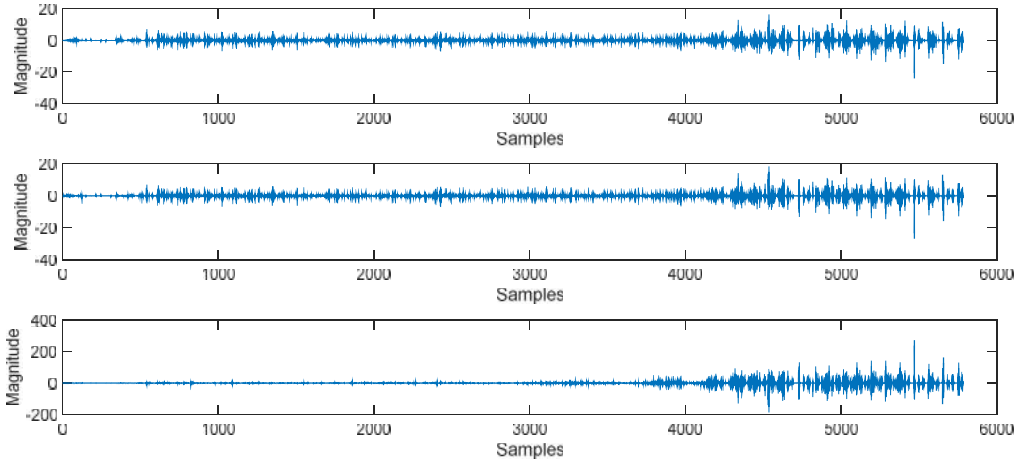

Figure 20. Detail-1 coefficient of three phase current of circuit-1 during phase- 'C1-g' fault at 50% from bus-1 at FIT=0.05 seconds, R_g = 5 and R_f = 2

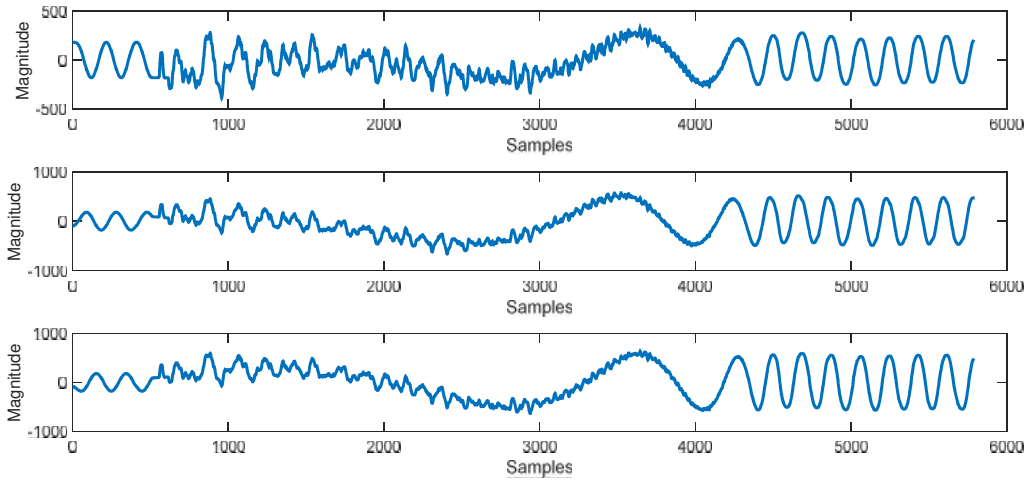

Figure 21. Approximate-1 coefficient of three phase current of circuit-2 during phase- 'C1-g' fault at 50% from bus-1 at FIT=0.05 seconds with $R_g = 5$ and $R_f = 2$

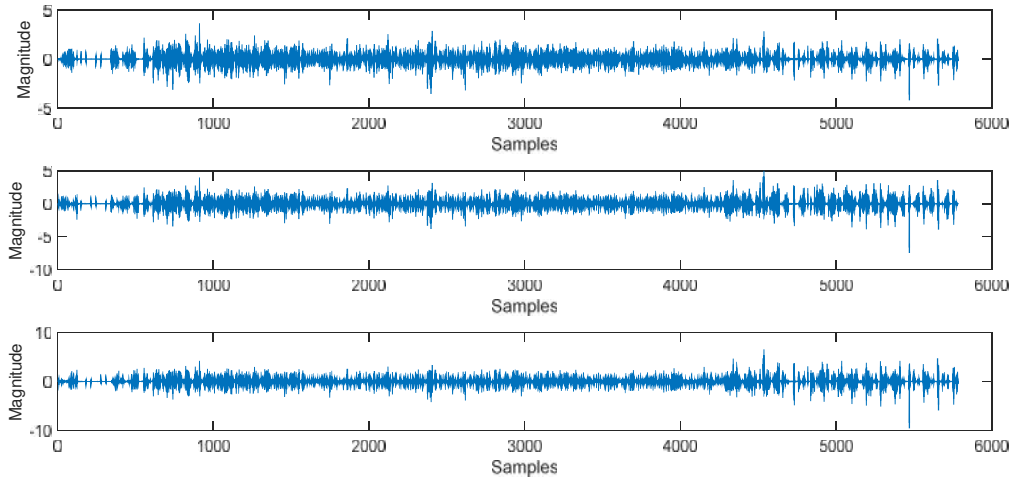

Figure 22. Detail-1 coefficient of three phase current of circuit-2 during phase- 'C1-g' fault at 50% from bus-1 at FIT=0.05 seconds with $R_g = 5$ and $R_f = 2$

Table 4. Test results of WT for phase-'C1-g' fault at 50% from bus-1 at FIT= 0.05 seconds with $R_g = 5$ and $R_f = 2$

Phase	Output		
	Approx. Coefficient	**Detail Coefficient**	**Wavelet Energy**
A1	1.5437*10^3	13.0795	99.9234
B1	1.6768*10^3	14.9629	99.9383
C1	**1.5196*10^4**	**237.3226**	**99.9874**
A2	328.5454	3.0674	99.0934
B2	570.4469	4.1420	99.7363
C2	641.3831	5.4063	99.7896

4.5 Performance During Inter-Circuit Faults: Inter circuit faults are the faults which occur in double circuit transmission lines and involve phases from both circuits. Inter circuit phase- 'A1A2-g' fault case at 50% at FIT=0.05 seconds is simulated to evaluate the performance of the proposed fault detection technique. The three phase current of circuit-1 and circuit-2 during phase-'A1A2-g' inter-circuit fault at 50% from bus-1 at FIT=0.05 seconds with $R_f = R_g = 0.001$ are depicted in Figure 23. The approximate-1 and detail-1 coefficients of three phase current of circuit-1 and circuit-2 for phase-'A1A2-g' fault can be seen in Figures 24-27. Table 5

depicts the test result for phase-'A1A2-g' fault. Thus, the inter-circuit fault is correctly detected and the faulty phases are correctly identified with the help of proposed technique.

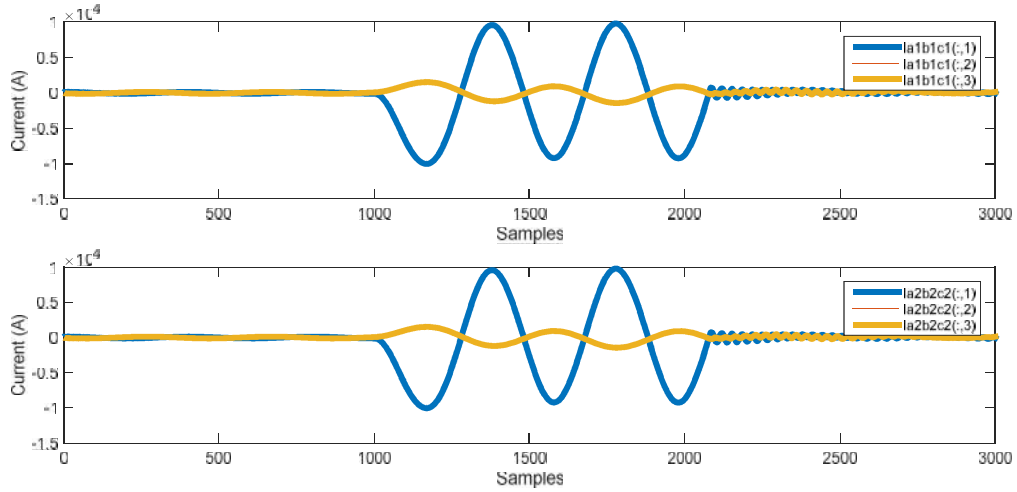

Figure 23. Three phase current of circuit-1 and circuit-2 during phase-'A1A2-g' inter-circuit fault at 50% from bus-1 at FIT=0.05 seconds with $R_f = R_g = 0.001$

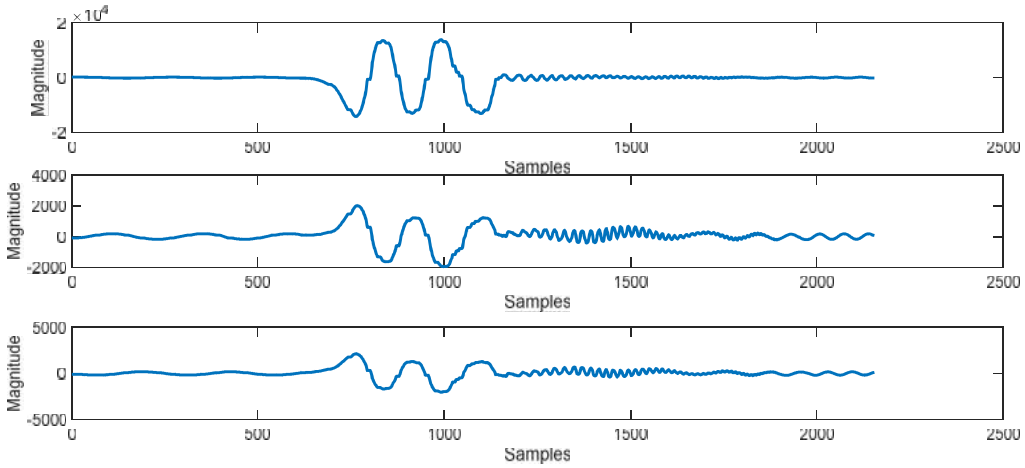

Figure 24. Approximate-1 coefficient of three phase current of circuit-1 during phase-'A1A2-g' inter-circuit fault at 50% from bus-1 at FIT=0.05 seconds with $R_f = R_g = 0.001$

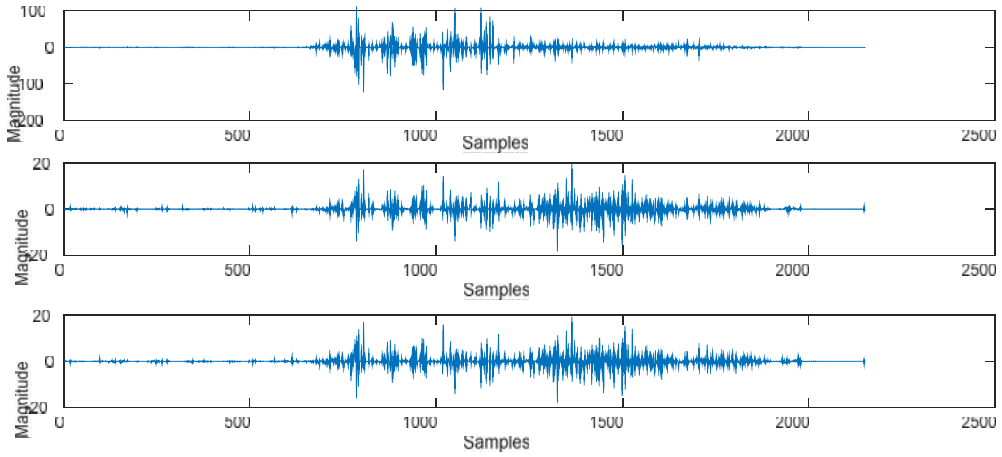

Figure 25. Detail-1 coefficient of three phase current of circuit-1 during phase-'A1A2-g' inter-circuit fault at 50% from bus-1 at FIT=0.05 seconds with $R_f = R_g = 0.001$

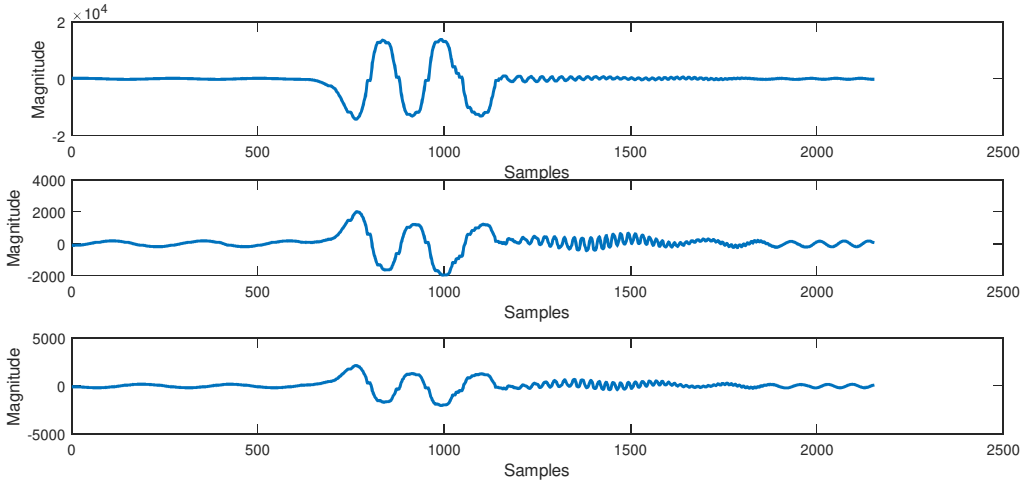

Figure 26. Approximate-1 coefficient of three phase current of circuit-2 during phase-'A1A2-g' inter-circuit fault at 50% from bus-1 at FIT=0.05 seconds with $R_f = R_g = 0.001$

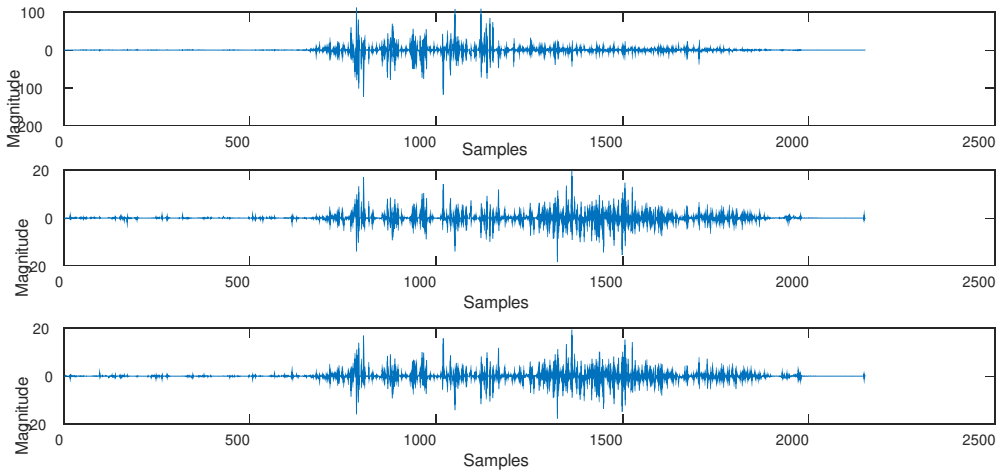

Figure 27. Detail-1 coefficient of three phase current of circuit-2 during phase-'A1A2-g' inter-circuit fault at 50% from bus-1 at FIT=0.05 seconds with $R_f = R_g = 0.001$

Table 5. Test results of WT for phase-'A1A2-g' inter-circuit fault at 50% from bus-1 at FIT=0.05 seconds with $R_f = R_g = 0.001$

Phase	Output		
	Approx. Coefficient	Detail Coefficient	Wavelet Energy
A1	**1.3862*10^4**	**97.6881**	**99.2546**
B1	2.0142*10^3	17.4854	96.6498
C1	2.1463*10^3	17.0579	96.9183
A2	**1.3862*10^4**	**97.6881**	**99.2546**
B2	2.0142*10^3	17.4854	96.6498
C2	2.1463*10^3	17.0579	96.9183

4.6 Performance During Cross-Country Faults: Simulation studies are conducted to examine the performance of the proposed scheme during phase-'B1-g' and phase-'A1C1-g' cross-country fault at 35% and 65% from bus-1 at FIT= 0.1 seconds with $R_f = R_g = 1$. The three phase current of circuit-1 and circuit-2 during phase-'B1-g' and phase-'A1C1-g' cross-country fault at 35% and 65% from bus-1 are depicted in Figure 28. The approximate-1 and detail-1 coefficients of three phase current of circuit-1 and circuit-2 during phase-'B1-g' and phase-'A1C1-g' cross-country fault can be seen in Figures 29-32. The output of wavelet transform based fault detection technique during phase-'B1-g' and phase-'A1C1-g' cross-country fault at 35% and 65% from bus-1 is outlined in Table 6. Thus, the proposed technique effectively detects the cross country faults.

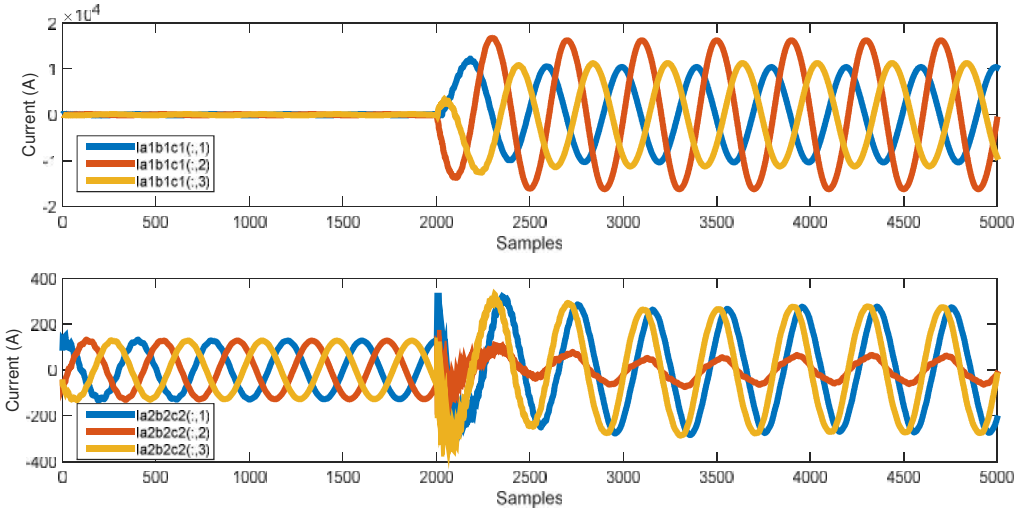

Figure 28. Three phase current of circuit-1 and circuit-2 during phase-'B1-g' and phase-'A1C1-g' cross-country fault at 35% and 65% from bus-1 at FIT= 0.1 seconds with $R_f = R_g = 1$

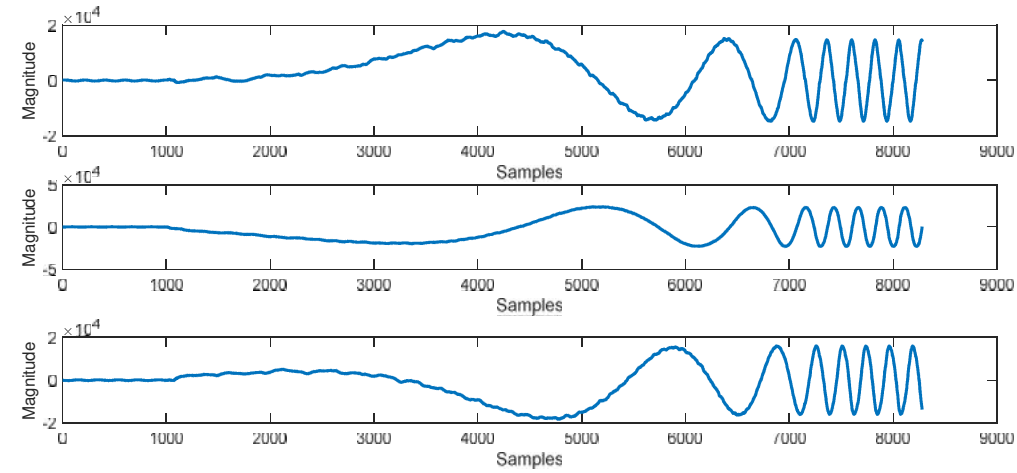

Figure 29. Approximate-1 coefficient of three phase current of circuit-1 during phase- 'B1-g' and phase-'A1C1-g' cross-country fault at 35% and 65% from bus-1 at FIT= 0.1 seconds with $R_f = R_g = 1$

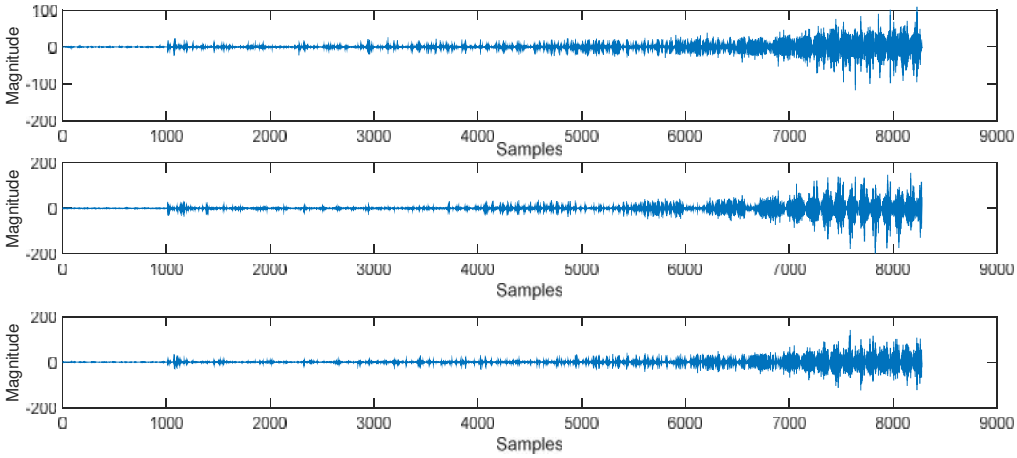

Figure 30. Detail-1 coefficient of three phase current of circuit-1 during phase- 'B1-g' and phase-'A1C1-g' cross-country fault at 35% and 65% from bus-1 at FIT= 0.1 seconds with $R_f = R_g = 1$

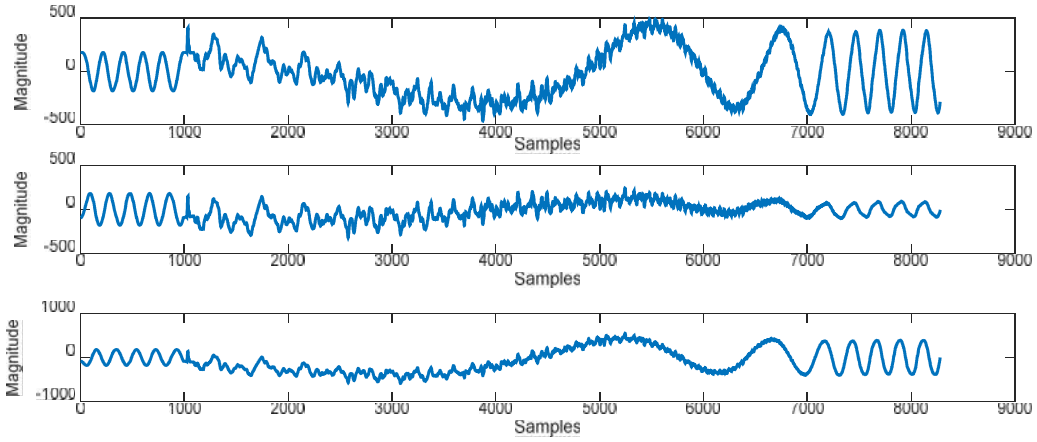

Figure 31. Approximate-1 coefficient of three phase current of circuit-2 during phase- 'B1-g' and phase-'A1C1-g' cross-country fault at 35% and 65% from bus-1 at FIT= 0.1 seconds with $R_f = R_g = 1$

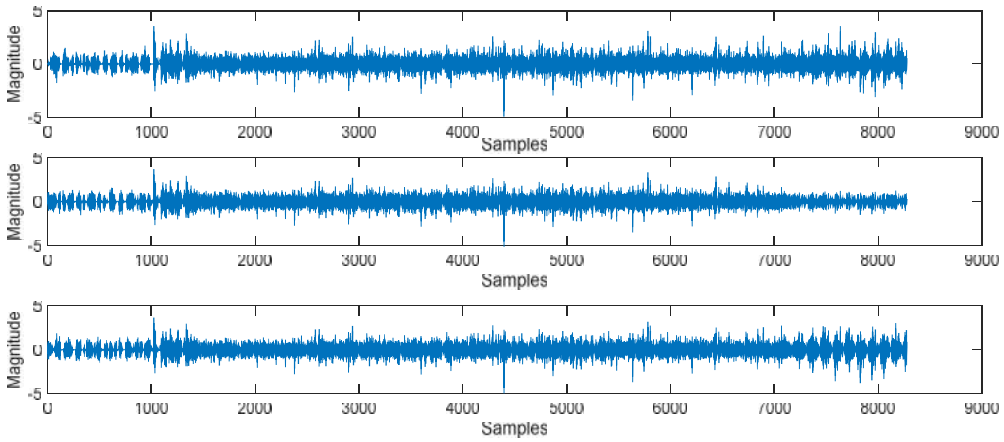

Figure 32. Detail-1 coefficient of three phase current of circuit-2 during phase- 'B1-g' and phase-'A1C1-g' cross-country fault at 35% and 65% from bus-1 at FIT= 0.1 seconds with $R_f = R_g = 1$

Table 6. Test results of WT for phase-'B1-g' and phase-'A1C1-g' cross-country fault at 35% and 65% from bus-1 at FIT= 0.1 seconds with $R_f = R_g = 1$

Phase	Output		
	Approx. Coefficient	Detail Coefficient	Wavelet Energy
A1	**1.7826*10^4**	**94.0805**	**99.9902**
B1	**2.3870*10^4**	**130.9622**	**99.9929**
C1	**1.6037*10^4**	**116.9069**	**99.9893**
A2	493.7247	3.0593	99.6293
B2	242.8469	3.0776	98.2310
C2	551.8693	3.0413	99.7504

4.7 Performance During Close-in Faults: It is very significant to evaluate the performance of any fault detection technique for a close-in fault. The fault detector should operate correctly for a close-in fault and it should accurately identify the faulty phases. The performance of the proposed method is analyzed during phase-'B1C1' fault at 9% from bus-1 with $R_f = 12$ at FIT=0.15 seconds. The three phase current of circuit-1 and circuit-2 during phase-'B1C1' fault at 9% from bus-1 with $R_f = 12$ at FIT=0.15 seconds are depicted in Figure 33. The approximate-1 and detail-1 coefficients of three phase current of circuit-1 and circuit-2 during phase-'B1C1' fault at 9% from bus-1 can be seen in Figures 34-37. Further, Table 7 depicts the output of the fault detector for phase-'B1C1' fault simulated at 9% from the relay location. It can be concluded that the fault detector correctly detects the close-in relay fault and identifies the faulty phase accurately with 100% accuracy.

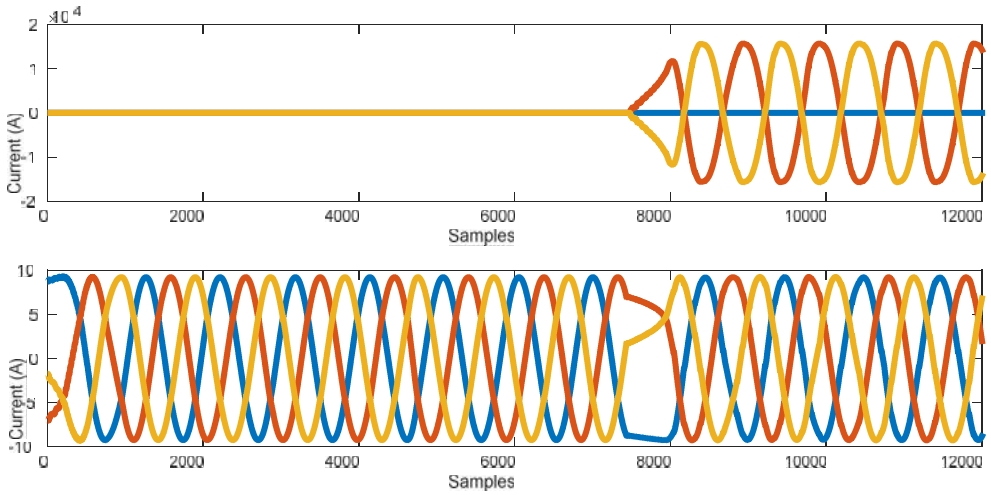

Figure 33. Three phase current of circuit-1 and circuit-2 during phase-'B1C1' fault at 9% from bus-1 at FIT=0.15 seconds with $R_f = 12$

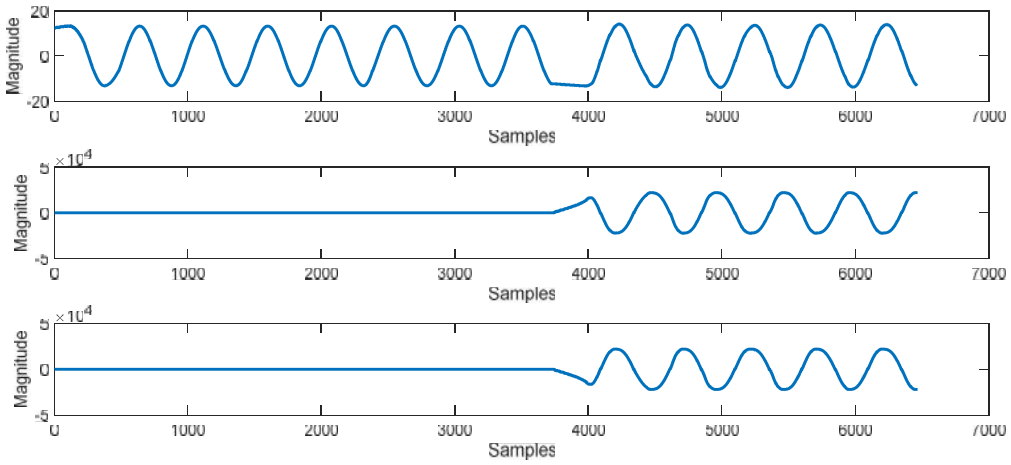

Figure 34. Approximate-1 coefficient of three phase current of circuit-1 during phase- 'B1C1' fault at 9% from bus-1 at FIT=0.15 seconds with $R_f = 12$

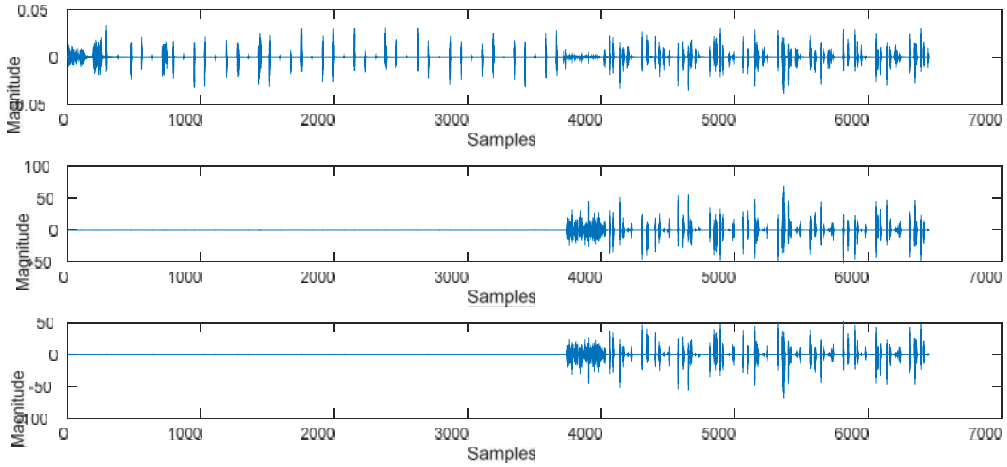

Figure 35. Detail-1 coefficient of three phase current of circuit-1 during phase- 'B1C1' fault at 9% from bus-1 at FIT=0.15 seconds with $R_f = 12$

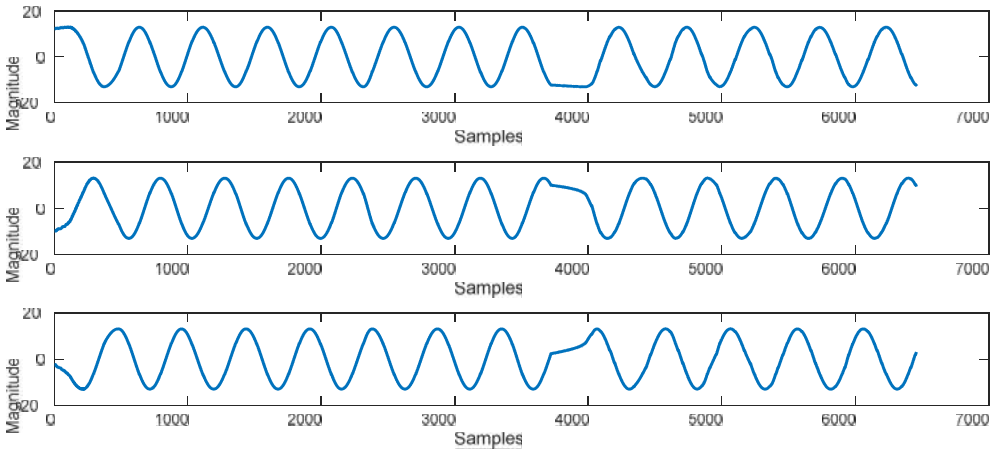

Figure 36. Approximate-1 coefficient of three phase current of circuit-2 during phase- 'B1C1' fault at 9% from bus-1

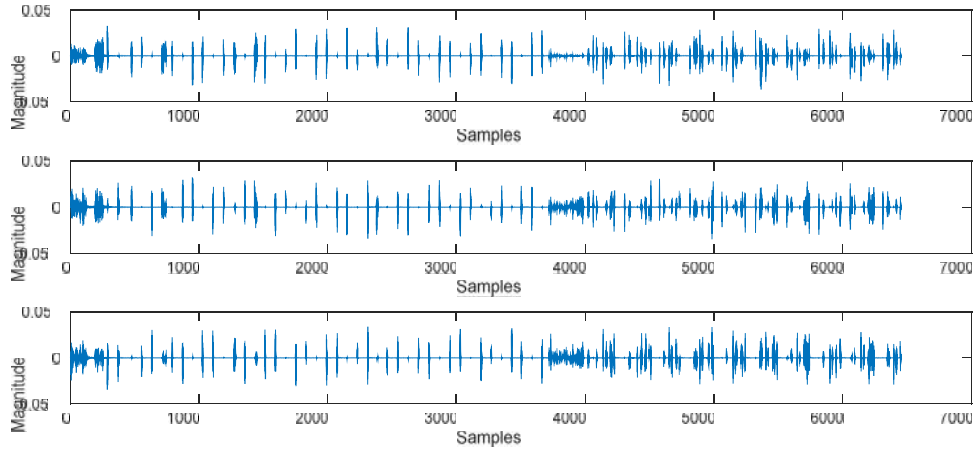

Figure 37. Detail-1 coefficient of three phase current of circuit-2 during phase- 'B1C1' fault at 9% from bus-1

Table 7. Test results of WT for phase-'B1C1' fault at 9% from bus-1 at FIT=0.15 seconds with R_f = 12

Phase	Output		
	Approx. Coefficient	Detail Coefficient	Wavelet Energy
A1	14.1023	0.0280	99.9982
B1	**2.2192*10^4**	**60.2382**	**99.9958**
C1	**2.2180*10^4**	**43.6208**	**99.9958**
A2	13.1676	0.0271	99.9982
B2	13.0897	0.0265	99.9982
C2	13.0877	0.0279	99.9979

4.8 Performance During Remote-end Faults: It is very significant to evaluate the performance of any fault detection technique for remote-end faults because there is a chance of the relay to under reach during a remote-end fault. The fault detector should operate correctly for a remote-end fault and should accurately identify the faulty phases. To evaluate the performance of the proposed fault detection technique under this type of situation, a four phase to ground fault phase-'B1A2B2C2-g' at 95% from bus-1 at 0.1 seconds with R_f = 20 and R_g = 45 is simulated, and the simulation result is depicted in Figure 38. The approximate-1 and detail-1 coefficients of three phase current of circuit-1 and circuit-2 during phase-'B1A2B2C2-g' fault at 95% from bus-1 can be seen in Figures 39-42. Further, Table 8 depicts the output of fault detector for phase-'B1A2B2C2-g' fault simulated at 95% from the relay location. It can be concluded that the fault detector correctly detects the far-end relay fault and identifies the faulty phase accurately with 100% accuracy.

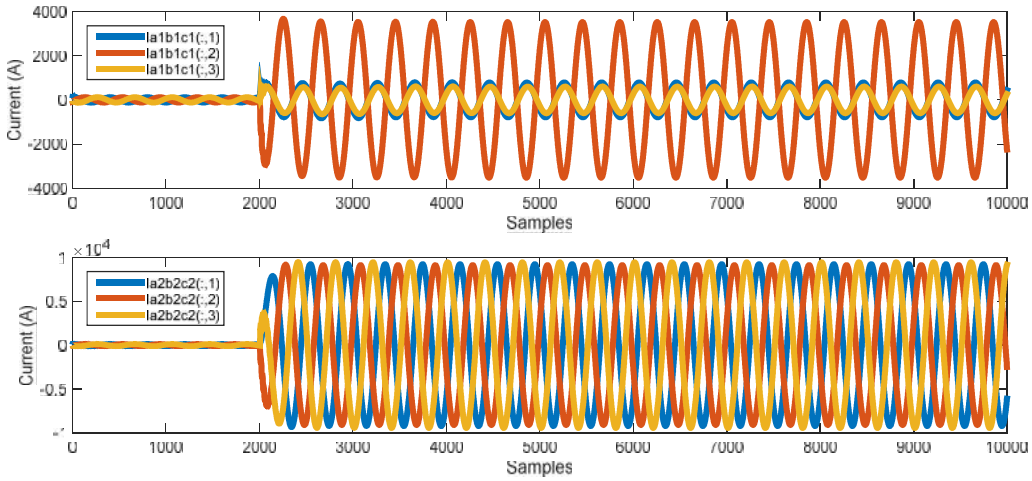

Figure 38. Three phase current of circuit-1 and circuit-2 during phase-'B1A2B2C2-g' fault at 95% from bus-1 with $R_f = 20$, $R_g = 45$ at FIT=0.1 seconds

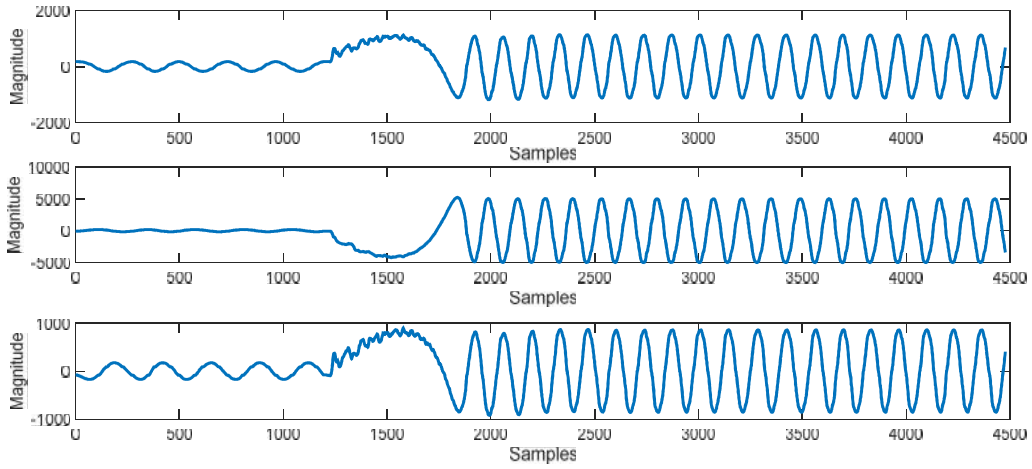

Figure 39. Approximate-1 coefficient of three phase current of circuit-1 during phase- 'B1A2B2C2-g' fault at 95% from bus-1 with $R_f = 20$, $R_g = 45$ at FIT=0.1 seconds

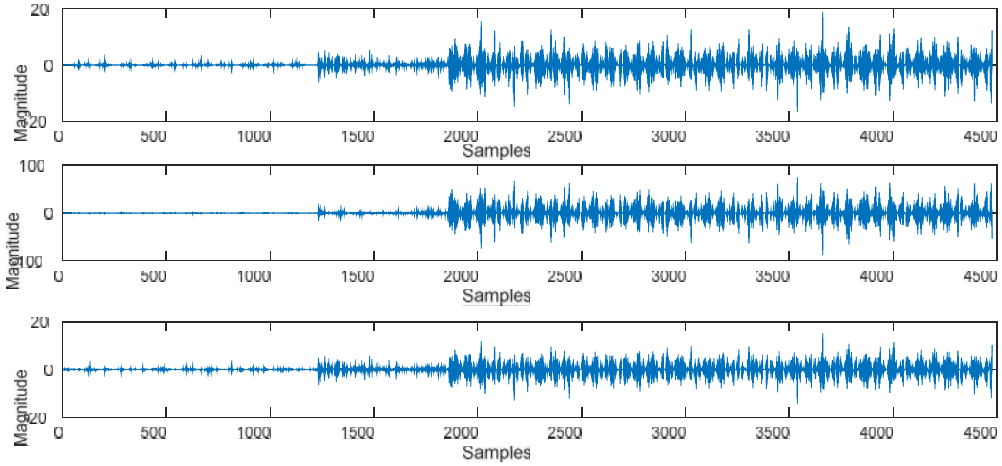

Figure 40. Detail-1 coefficient of three phase current of circuit-1 during phase- 'B1A2B2C2-g' fault at 95% from bus-1 with $R_f = 20$, $R_g = 45$ at FIT=0.1 seconds

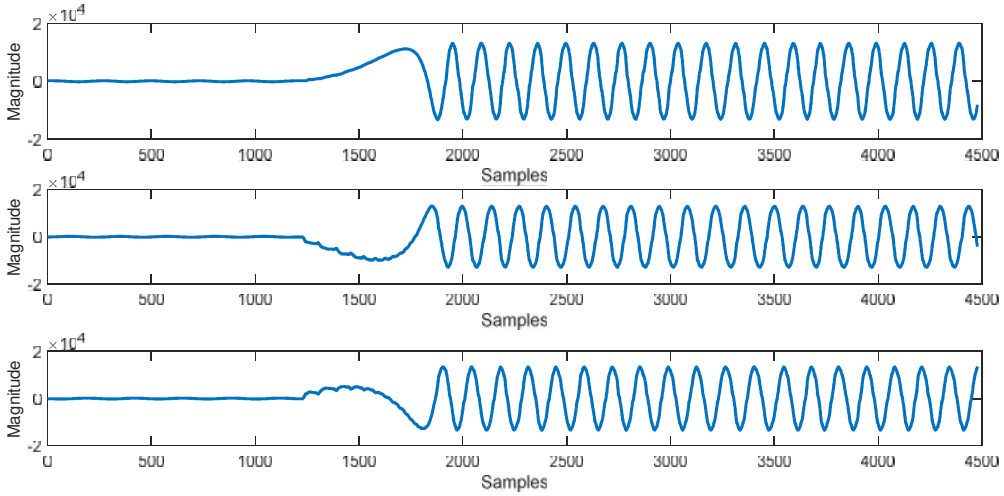

Figure 41. Approximate-1 coefficient of three phase current of circuit-2 during phase- 'B1A2B2C2-g' fault at 95% from bus-1 with $R_f = 20$, $R_g = 45$ at FIT=0.1 seconds

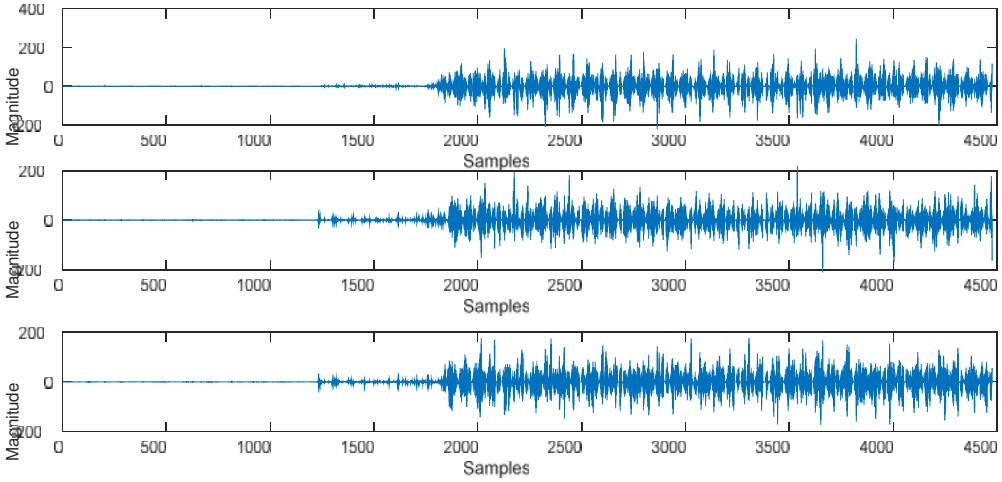

Figure 42. Detail-1 coefficient of three phase current of circuit-2 during phase- 'B1A2B2C2-g' fault at 95% from bus-1 with $R_f = 20$, $R_g = 45$ at FIT=0.1 seconds

Table 8. Test results of WT for phase-'B1A2B2C2-g' fault at 95% from bus-1 with $R_f = 20$, $R_g = 45$ at FIT=0.1 seconds

Phase	Output		
	Approx. Coefficient	Detail Coefficient	Wavelet Energy
A1	1.1277*10^3	16.9341	99.8503
B1	**5.2047*10^3**	**63.3939**	**99.8642**
C1	898.4127	12.8559	99.8270
A2	**1.3061*10^4**	**217.0467**	**99.8207**
B2	**1.3001*10^4**	**196.2669**	**99.8371**
C2	**1.3384*10^4**	**154.0546**	**99.8604**

5. Conclusions

Wavelet transform based fault detection and faulty phase identification technique is found to be very effective under numerous fault conditions. The robustness of the proposed technique is not affected by various fault situations viz. varying fault type, fault resistance, ground resistance, fault location and fault inception time. Test results depicts that the proposed technique effectively

detects the fault and identifies the faulty phase perfectly. The main benefit of using this technique for the purpose of fault detection and classification on series capacitor compensated double circuit transmission line is that this technique uses the samples of three phase currents of both the circuits measured at only one end of the SCCDCTL.

References

Biswal S., Biswal M. and Malik O. P., 2018. Hilbert Huang transform based online differential relay algorithm for shunt compensated transmission line, *EEE Transactions on Power Delivery*, Vol. 33, No. 6, pp. 2803-2811.

Biswas S., Kumar K., Ghosal A. and Nayak P. K., 2018. Fault detection and classification for TCSC compensated transmission lines using wavelet energy, *Proc. 4th IEEE International Conference on Recent Advances on Information Technology (RAIT),* pp. 1-5.

Gaur V. K. and Bhalja B., 2018. New fault detection and localization technique for double-circuit three-terminal transmission line, *IET Generation, Transmission & Distribution*, Vol.12, No.8, pp. 1687-1696.

Gautam N., Kapoor G., Ali S., 2018. Wavelet transform based technique for fault detection and classification in a 400 kV double circuit transmission line, *Asian Journal of Electrical Sciences*, Vol. 7, No. 2, pp. 77-83.

Gautam N., Ali S. and Kapoor G., 2018. Detection of fault in series capacitor compensated double circuit transmission line using wavelet transform, *Proc. IEEE International Conference on Computing, Power and Communication Technologies (GUCON)*, pp. 769-773.

Govar S. A. and Seyedi H., 2016. Adaptive CWT-based transmission line differential protection scheme considering cross-country faults and CT saturation, *IET Generation, Transmission & Distribution*, Vol. 10, No.9, pp. 2035-2041.

Kang N., Chen J., and Liao Y., 2015. A Fault-location algorithm for series-compensated double-circuit transmission lines using the distributed parameter line model, *IEEE Transactions on Power Delivery*, Vol.30, No.1, pp. 360-367.

Kapoor G., 2018. Mathematical morphology based fault detector for protection of double circuit transmission line, *ICTACT Journal on Microelectronics*, Vol.4, No.2, pp. 589-600.

Koley E., Kumar R., and Ghosh S., 2016. Low cost microcontroller based fault detector, classifier, zone identifier and locator for transmission lines using wavelet transform and artificial neural network: A hardware co-simulation approach, *International Journal of Electrical Power and Energy Systems*, Vol.81, pp. 346-360.

Kapoor G., 2018. Wavelet transform based fault detector for protection of series capacitor compensated three phase transmission line, *International Journal of Engineering, Science and Technology*, Vol. 10, No. 4, pp. 29-49.

Kapoor G., 2018. Protection scheme for double circuit transmission lines based on wavelet transform, *ICTACT Journal on Microelectronics*, Vol. 4, No. 3, pp. 656-664.

Koley E., Shukla S. K., Ghosh S., Mohanta D. K., 2017. Protection scheme for power transmission lines based on SVM and ANN considering the presence of non-linear loads, *IET Generation, Transmission & Distribution*, Vol.11, No.9, pp. 2333-2341.

Monteiro B. C. R., Jr. F. M., Lopes F. V. and Silva K. M., 2018. Cross-differential protection for double-circuit lines using current travelling waves, *Proc. IEEE International Conference, Simposio Brasileiro de Sistemas Eletricos (SBSE),* pp. 1-6.

Nagam S. S., Koley E., Ghosh S., 2017. Artificial neural network based fault locator for three phase transmission line with STATCOM, *Proc. IEEE International Conference on Computational Intelligence and Computing Research (ICCIC)*, pp. 1-4.

Swetapadma A. and Yadav A., 2016. Protection of parallel transmission lines including inter-circuit faults using Naïve Bayes classifier, *Alexandria Engineering Journal*, Vol.55, No.2, pp. 1411-1419.

Saravanan N. and Rathinam A., 2012. A comparative study on ANN based fault location and classification technique for double circuit transmission line, *Proc. 4th IEEE International Conference on Computational Intelligence and Communication Networks*, pp. 824-830.

Swetapadma A. and Yadav A., 2016. Time domain complete protection scheme for parallel transmission lines, *Ain Shams Engineering Journal*, Vol.7, No.1, pp. 169-183.

Yadav A. and Swetapadma A., 2014. Improved first zone reach setting of artificial neural network-based directional relay for protection of double circuit transmission lines, *IET Generation, Transmission & Distribution*, Vol.8, No.3, pp. 373-388.

Biographical notes

Gaurav Kapoor received B.E. in Electrical Engineering from University of Rajasthan, Jaipur, India and M. Tech. in Power System specialization from University College of Engineering, Rajasthan Technical University, Kota, India in 2011 and 2014, respectively. He is an Assistant Professor in the Department of Electrical Engineering, Modi Institute of Technology Kota, India. He has published more than forty papers in various journals. He has also presented many research papers in national and international conferences. His research interests include power system digital protection.

Received December 2018
Accepted December 2018
Final acceptance in revised form December 2018